DOI: 10.1021/ic900339u

Inorganic Chemistry
Article

Syntheses and Structures of Blue-Luminescent Mercury(II) Complexes with 2,6-Bis(imino)pyridyl Ligands

Ruiqing Fan,*,† Yulin Yang,*,† Yanbin Yin,† WuLiJi Hasi,† and Ying Mu‡

†*Department of Chemistry, Harbin Institute of Technology, Harbin 150001, P. R. of China, and*
‡*Key Laboratory for Supramolecular Structure and Materials of Ministry of Education, School of Chemistry, Jilin University, Changchun 130012, P. R. of China*

Received February 20, 2009

Seven five-coordinate 2,6-bis(imino)pyridyl mercury complexes, [2,6-(ArN═CMe)$_2$C$_5$H$_3$NHgCl$_2$·*n*CH$_3$CN] (Ar = C$_6$H$_5$, *n* = 1.5, **1**; Ar = 2,6-^{i}Pr$_2$C$_6$H$_3$, *n* = 0, **2**; Ar = 2,6-Me$_2$C$_6$H$_3$, *n* = 1, **3**; Ar = 2-MeC$_6$H$_4$, *n* = 1, **4**; Ar = 4-MeC$_6$H$_4$, *n* = 1, **5**; Ar = 2,4,6-Me$_3$C$_6$H$_2$, *n* = 1, **6**; Ar = 2,6-Et$_2$C$_6$H$_3$, *n* = 0, **7**), were synthesized by reactions of the corresponding bis(imino)pyridine ligands with HgCl$_2$ in CH$_3$CN, and in good yield. The structures of complexes **1**−**6** were determined by single-crystal X-ray diffraction. In all complexes, the metal center is tridentately chelated by the ligand and further coordinated by two chlorine atoms, resulting in a distorted trigonal bipyramidal geometry. All complexes have blue luminescence at room temperature in solution and the solid state. At 293 K in a CH$_2$Cl$_2$ solution, the fluorescent emission maxima for complexes **1**−**7** are at λ = 395, 400, 407, 403, 427, 415, and 403 nm, respectively, which can be attributed to ligand-centered $\pi^* \rightarrow \pi$ transitions.

Introduction

Luminescent coordination compounds with nitrogen-containing ligands have attracted much attention recently due to their good performance in sensor technologies and electroluminescent devices.[1−11] For example, luminescent noble

*To whom correspondence should be addressed. Fax: +86-451-86418270. E-mail: fanruiqing@163.com (R.F.), and ylyang@hit.edu.cn (Y.Y.).

(1) (a) Yu, G.; Yin, S. W.; Liu, Y. Q.; Shuai, Z. G.; Zhu, D. B. *J. Am. Chem. Soc.* **2003**, *125*, 14816. (b) Berry, S. M.; Bebout, D. C. *Inorg. Chem.* **2005**, *44*, 27. (c) Aragoni, M. C.; Arca, M.; Demartin, F.; Devillanova, F. A.; Lsaia, F.; Garau, A.; Lippolis, V.; Jalali, F.; Papke, U.; Shamsipur, M.; Tei, L.; Yari, A.; Verani, G. *Inorg. Chem.* **2002**, *41*, 6623. (d) Xu, X. X.; Lu, Y.; Wang, E. B.; Ma, Y.; Bai, X. L. *Cryst. Growth Des.* **2006**, *6*, 2029. (e) Xu, X. X.; Lu, Y.; Wang, E. B.; Ma, Y.; Bai, X. L. *Inorg. Chim. Acta* **2007**, *360*, 455. (f) Liu, Q. D.; Wang, R. Y.; Wang, S. N. *J. Chem. Soc., Dalton Trans.* **2004**, 2073.

(2) (a) Li, X. P.; Zhang, J. Y.; Liu, Y.; Pan, M.; Zheng, S. R.; Kang, B. S.; Su, C. Y. *Inorg. Chim. Acta* **2007**, *360*, 2990. (b) Jin, F.; Zhou, H.-P.; Wang, X.-C.; Hu, Z.-J.; Wu, J.-Y.; Tian, Y.-P.; Jiang, M.-H. *Polyhedron* **2007**, *26*, 1338. (c) Bazzicalupi, C.; Bencini, A.; Berni, E.; Bianchi, A.; Borsari, L.; Giorgi, C.; Valtancoli, B.; Lodeiro, C.; Lima, J. C.; Parola, A. J.; Pina, F. J. *Chem. Soc., Dalton Trans.* **2004**, 591. (d) Shao, K.-Z.; Zhao, Y.-H.; Wang, X.-L.; Lan, Y.-Q.; Wang, D.-J.; Su, Z.-M.; Wang, R.-S. *Inorg. Chem.* **2009**, *48*, 10.

(3) (a) Wu, Q.; Lavigne, J. A.; Tao, Y.; D'Iorio, M.; Wang, S. *Inorg. Chem.* **2000**, *39*, 5248. (b) Yam, V. W. W.; Pui, Y. L.; Wong, K. M. C.; Cheung, K. K. *J. Chem. Soc. Chem. Commun.* **2000**, 1751. (c) Yang, W.; Schmider, H.; Wu, Q.; Zhang, Y. S.; Wang, S. *Inorg. Chem.* **2000**, *39*, 2397. (d) Wong, W. Y.; Tsang, K. Y.; Tam, K. H.; Lu, G. L.; Sun, C. *J. Organomet. Chem.* **2000**, *601*, 237. (e) Sazanovich, L. V.; Kirmaier, C.; Hindin, E.; Yu, L.; Bocian, D. F.; Lindsey, J. S.; Holten, D. *J. Am. Chem. Soc.* **2004**, *126*, 2664. (f) Chen, X.-L.; Gou, L.; Hu, H.-M.; Fu, F.; Han, Z.-X.; Shu, H.-M; Yang, M.-L.; Xue, G.-L.; Du, C.-Q. *Eur. J. Inorg. Chem.* **2008**, 239.

(4) (a) Anjali, K. S.; Pui, Y. L.; Yam, V. W. W.; Vittal, J. J. *Inorg. Chim. Acta* **2001**, *319*, 57. (b) Zhu, H.; Ströbele, M.; Yu, Z.; Wang, Z.; Meyer, H. J.; You, X. *Inorg. Chem. Commun.* **2001**, *4*, 577. (c) Kang, Y.; Seward, C.; Song, D.; Wang, S. *Inorg. Chem.* **2003**, *42*, 2789. (d) Yam, V. W. W.; Pui, Y. L.; Cheung, K. K. *New J. Chem.* **1999**, *23*, 1163. (e) Du, M.; Li, C. P.; Zhao, X. J.; Yu, Q. *CrystEngComm* **2007**, *9*, 1011.

(5) (a) Yam, V. W. W.; Pui, Y. L.; Cheug, K. K. *J. Chem. Soc., Dalton Trans.* **2000**, 3658. (b) Kunkely, H.; Vogler, A. *J. Photochem. Photobiol., A* **2001**, *144*, 69. (c) Das, S.; Hung, C.-H.; Goswami, S. *Inorg. Chem.* **2003**, *42*, 8592. (d) Atoub, N.; Mahmoudi, G.; Morsali, A. *Inorg. Chem. Commun.* **2007**, *10*, 166.

(6) (a) Niu, C.-Y.; Wu, B.-L.; Zheng, X.-F.; Zhang, H.-Y.; Hou, H.-W. *Cryst. Growth Des.* **2008**, *8*, 1566. (b) Chu, Z.-L; Zhu, H.-B.; Hu, D.-H.; Huang, W.; Gou, S.-H. *Cryst. Growth Des.* **2008**, *8*, 1599. (c) Ranjbar, Z. R.; Morsali, A. *Inorg. Chim. Acta* **2007**, *360*, 2056.

(7) (a) Tang, C. W.; VanSlyke, S. A. *Appl. Phys. Lett.* **1987**, *51*, 913. (b) Baldo, M. A.; Lamansky, S.; Burrows, P. E.; Thompson, M. E.; Forrest, S. R. *Appl. Phys. Lett.* **1999**, *75*, 4. (c) Adachi, C.; Kwong, R. C.; Djurovich, P.; Adamovich, V.; Baldo, M. A.; Thompson, M. E.; Forrest, S. R. *Appl. Phys. Lett.* **2001**, *79*, 2082.

(8) (a) Sprouse, S.; King, K. A.; Spellane, P. J.; Watts, R. J. *J. Am. Chem. Soc.* **1984**, *106*, 6647. (b) Balzani, V.; Juris, A.; Venturi, M.; Campagna, S.; Serroni, S. *Chem. Rev.* **1996**, *96*, 759. (c) Tian, A.-X.; Ying, J.; Peng, J.; Sha, J.-Q.; Pang, H.-J.; Zhang, P.-P.; Chen, Y.; Zhu, M.; Su, Z.-M. *Inorg. Chem.* **2009**, *48*, 100.

(9) (a) Jia, W. L.; Liu, Q. D.; Wang, R.; Wang, S. *Organometallics* **2003**, *22*, 4070. (b) Lamansky, S.; Djurovich, P.; Murphy, D.; Abdel-Razzag, F.; Lee, H. E.; Adachi, C.; Burrows, P. E.; Forrest, S. R.; Thompson, M. E. *J. Am. Chem. Soc.* **2001**, *123*, 4304.

(10) (a) Xia, H.; Zhang, C.; Liu, X.; Qiu, S.; Lu, P.; Shen, F.; Zhang, J.; Ma, Y. *J. Phys. Chem. B* **2004**, *108*, 3185. (b) Tung, Y. L.; Wu, P. C.; Liu, C. S.; Chi, Y.; Yu, J. K.; Hu, Y. H.; Chou, P. T.; Peng, S. M.; Lee, G. H.; Tao, Y.; Arthur, J. C.; Shu, C. F.; Wu, F. I. *Organometallics* **2004**, *23*, 3745. (c) Zhang, P.; Guo, J. H.; Wang, Y.; Pang, W. Q. *Mater. Lett.* **2002**, *53*, 400. (d) Tung, Y. L.; Lee, S. W.; Chi, Y.; Chen, L. S.; Shu, C. F.; Wu, F. I.; Carty, A. J.; Chou, P. T.; Peng, S. M.; Lee, G. H. *Adv. Mater.* **2005**, *17*, 1059.

(11) (a) Chen, Y. L.; Lee, S. W.; Chi, Y.; Hwang, K. C.; Kumar, S. B.; Hu, Y. H.; Cheng, Y. M.; Chou, P. T.; Peng, S. M; Lee, G. H.; Yeh, S. J.; Chen, C. T. *Inorg. Chem.* **2005**, *44*, 4287. (b) Carlson, B.; Phelan, G. D.; Kaminsky, W.; Dalton, L.; Jiang, X. Z.; Liu, S.; Jen, A. K.-Y. *J. Am. Chem. Soc.* **2002**, *124*, 14162. (c) Xia, H.; Zhang, C.; Qiu, S.; Lu, P.; Zhang, J.; Ma, Y. *Appl. Phys. Lett.* **2004**, *84*, 290.

Published on Web 06/03/2009

Table 1. Crystal Data and Structure Refinement for **1**−**6**

data	**1**	**2**	**3**	**4**	**5**	**6**
formula	$C_{24}H_{23.5}N_{4.5}Cl_2Hg$	$C_{33}H_{43}N_3Cl_2Hg$	$C_{27}H_{30}N_4Cl_2Hg$	$C_{25}H_{26}N_4Cl_2Hg$	$C_{25}H_{26}N_4Cl_2Hg$	$C_{29}H_{34}N_4Cl_2Hg$
fw	646.47	753.19	682.04	653.99	653.99	710.09
cryst syst	triclinic	triclinic	monoclinic	triclinic	monoclinic	monoclinic
space group	$P\bar{1}$	$P\bar{1}$	$P2_1/c$	$P\bar{1}$	$C2/c$	$P2_1/n$
a/Å	8.9830(18)	8.8470(18)	13.377(3)	9.3470(19)	21.8046(14)	16.826(5)
b/Å	12.591(3)	9.853(2)	14.863(3)	12.994(3)	14.8059(10)	14.980(4)
c/Å	22.783(5)	21.037(4)	14.499(3)	21.585(4)	16.8208(12)	23.598(6)
α/deg	92.14(3)	80.47(3)		93.59(3)		
β/deg	97.30(3)	88.41(3)	108.44(3)	90.64(3)	101.4770(10)	92.896(4)
γ/deg	93.55(3)	66.89(3)		98.18(3)		
volume (Å^3)	2548.4(9)	1662.0(6)	2735.0(10)	2589.3(9)	5321.8(6)	5941(3)
Z	2[a]	2	4	2[a]	4	4[a]
D_{calcd}, g cm^{-3}	1.685	1.505	1.656	1.678	0.816	1.588
μ, mm^{-1}	6.268	4.816	5.845	6.170	3.002	5.385
F(000)	1252	752	1336	1272	1272	2800
θ range for data collection	1.89−27.48°	2.28−27.48°	1.81−27.48°	0.95−27.48°	1.67−28.59°	1.61−26.14°
limiting indices	$-11 \le h \le 11$	$0 \le h \le 11$	$-17 \le h \le 17$	$-11 \le h \le 11$	$-22 \le h \le 28$	$-20 \le h \le 20$
	$-15 \le k \le 16$	$-11 \le k \le 12$	$-19 \le k \le 19$	$-16 \le k \le 16$	$-19 \le k \le 19$	$-18 \le k \le 14$
	$-29 \le l \le 29$	$-27 \le l \le 27$	$-18 \le l \le 18$	$-28 \le l \le 27$	$-19 \le l \le 21$	$-28 \le l \le 28$
absorption correction			semiempirical			
data/restraints/params	10288/12/548	7359/12 /362	6041/6/315	9842/28/572	6259/6/290	11585/12/651
goodness-of-fit on F^2	1.026	1.014	1.044	0.967	0.852	0.667
final R indices [$I > 2\sigma(I)$]						
R_1[b]	0.0589	0.0561	0.0579	0.0640	0.0398	0.0488
wR_2[c]	0.1329	0.1461	0.1479	0.1167	0.0753	0.0884
R indices (all data)						
R_1[b]	0.0982	0.0821	0.0732	0.1460	0.0718	0.1066
wR_2[c]	0.1511	0.1529	0.1625	0.1432	0.0837	0.1094
largest diff. peak/hole (e·Å^{-3})	2.399/−1.193	1.948/−1.596	2.150/−1.791	1.174/−0.769	1.606/−0.599	1.336/−1.434

[a] There are two crystallographically independent molecules in the asymmetric unit. [b] $R_1 = \sum||F_o| - |F_c||/\sum|F_o|$. [c] $wR_2 = [\sum[w\,(F_o^2 - F_c^2)^2]/\sum[\,w\,(F_o^2)^2]]^{1/2}$.

Scheme 1

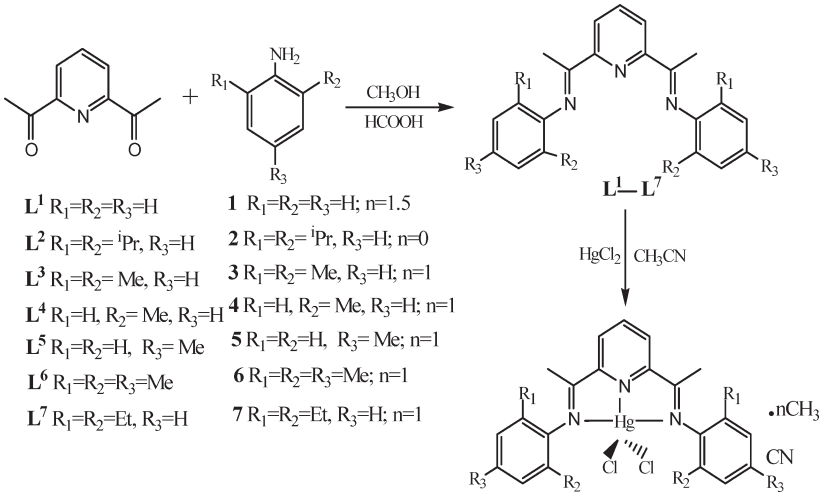

metal complexes with bipyridine-containing ligands have attracted much attention because of their high luminescent efficiency.[10,11] However, the lower synthetic yields and higher costs of these complexes are disadvantages for their use as optoelectronic materials. Lower-cost d^{10} metal complexes with nitrogen-containing ligands have been synthesized and their luminescent behavior studied,[1−6] among which, a few mercury complexes have been reported in studies concerning their luminescence behavior.[2,5] It has been found that, for a given complex, the size of the π-conjugated system of the ligand and the electronic effect of substituents on the ligand are important factors for modulating its luminescent properties.[3e,4c,4d] On the other hand, the design and synthesis of efficient luminescent chelating Hg(II) complexes is also of importance for detection of Hg(II), as mercury and its derivatives are highly toxic contaminants of the environment.[12] In the past several years, iron and cobalt complexes with bulky aryl-substituted

(12) (a) Guo, X. F.; Qian, X. H.; Jia, L. H. *J. Am. Chem. Soc*. **2004**, *126*, 2272. (b) Yu, Y.; Lin, L.-R.; Yang, K.-B.; Zhong, X.; Huang, R.-B.; Zheng, L.-S. *Talanta* **2006**, *69*, 103. (c) Wang, L.; Zhu, X.- J.; Wong, W.-Y.; Guo, J.-P.; Wong, W.-K.; Li, Z.-Y. *J. Chem. Soc., Dalton Trans*. **2005**, 3235.

(13) (a) Fan, R. Q.; Zhu, D. S.; Mu, Y.; Li, G. H.; Yang, Y. L.; Su, Q.; Feng, S. H. *Eur. J. Inorg. Chem*. **2004**, 4891. (b) Fan, R. Q.; Zhu, D. S.; Mu, Y.; Su, Q.; Xia, H. *Synth. Met*. **2005**, *149*, 135. (c) Fan, R. Q.; Zhu, D. S.; Mu, Y; Li, G. H.; Su, Q.; Ni, J. G.; Feng, S. H. *Chem. Res. Chin. Univ*. **2005**, *21*, 496.

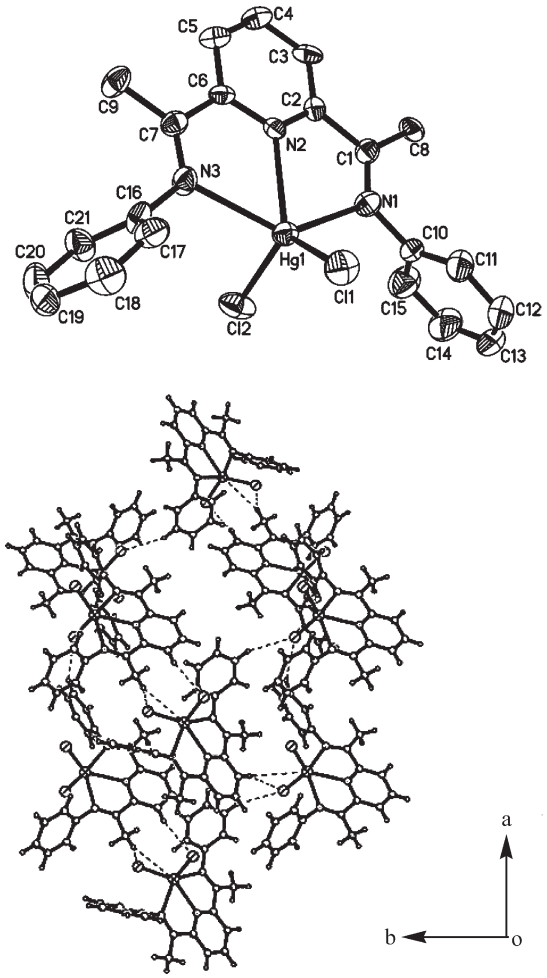

Figure 1. Top: Molecular structure of complex **1** (the other molecule and CH_3CN molecules have been omitted for clarity). Bottom: Packing diagram of complex **1** along the *c* axis. Hydrogen bonds are indicated by dashed lines.

bis(imino)pyridyl ligands were reported by Brookhart et al. and Gibson et al.[14−16] These iron and cobalt complexes exhibit high activity for olefin polymerization. Recently, we synthesized a number of bis(imino)pyridine zinc(II) and cadmium(II) complexes and explored the electronic effect of substituents at the aryl-ring of the bis(imino)pyridyl ligand on the luminescent properties of these complexes.[13] To fulfill full-color electroluminescent displays, three color components, that is, red, green, and blue, must be available. Stable blue luminescent compounds used for electroluminescent devices are still rare and very challenging to prepare. In this work, we report the syntheses, structures, and blue luminescent properties of seven new mercury(II) complexes with 2,6-bis(imino)pyridyl ligands, 2,6-$(ArN{=}CMe)_2C_5H_3NHgCl_2\cdot nCH_3CN$ (Ar = C_6H_5, n = 1.5, **1**; Ar = 2,6-$^i Pr_2C_6H_3$, n = 0, **2**; Ar = 2,6-$Me_2C_6H_3$, n = 1, **3**; Ar = 2-MeC_6H_4, n = 1, **4**; Ar = 4-MeC_6H_4, n = 1, **5**; Ar = 2,4,6-$Me_3C_6H_2$, n = 1, **6**; Ar = 2,6-$Et_2C_6H_3$, n = 0, **7**).

Experimental Section

Materials and Methods. All manipulations of air- and moisture-sensitive compounds were performed under an atmosphere of nitrogen using standard Schlenk techniques. ^{1}H NMR spectra were recorded on a Varian Mercury 300 MHz spectrometer. IR spectra were recorded on a Nicolet Impact 410 FTIR spectrometer using KBr pellets. Elemental analyses were performed on a Perkin-Elmer 240c element analyzer. UV−vis spectra were obtained on a Perkin-Elmer Lambda 20 spectrometer. Luminescence spectra were measured on a Perkin-Elmer LS55 Luminescence spectrometer at room temperature. Fluorescence lifetimes were measured with a Lecroy Wave Runner 6100 Digital Oscilloscope (1 GHz) using a 350 nm laser (pulse width = 4 ns) as the excitation source (Continuum Sunlite OPO). Solvents were refluxed over an appropriate drying agent and distilled and degassed prior to use. Aniline, 2,6-diisopropylaniline, 2,6-dimethylaniline, 2-methylaniline, 4-methylaniline, 2,4,6-trimethylaniline, and 2,6-diethylaniline were purchased from Aldrich Chemical Company and used as received. 2,6-Diacetylpyridine was prepared according to a published procedure.[18] Free ligands, 2,6-$(ArN{=}CMe)_2C_5H_3N$ [Ar = C_6H_5, L^1; Ar = 2,6-$^i Pr_2C_6H_3$, L^2; Ar = 2,6-$Me_2C_6H_3$, L^3; Ar = 2-MeC_6H_4, L^4; Ar = 4-MeC_6H_4, L^5; Ar = 2,4,6-$Me_3C_6H_2$, L^6; Ar = 2,6-$Et_2C_6H_3$, L^7] were synthesized according to published procedures in good yield by the condensation of 2,6-diacetylpyridine with the corresponding aniline in refluxing absolute methanol in the presence of a catalytic amount of formic acid (Scheme 1).[13,14]

Syntheses. Synthesis of 2,6-Bis[(1-phenylimino)ethyl]pyridineHgCl$_2\cdot$1.5CH$_3$CN (1). A mixture of L^1 (113 mg, 0.36 mmol) and $HgCl_2$ (98 mg, 0.36 mmol) in CH_3CN (20 mL) was stirred under nitrogen at room temperature for 12 h. Evaporation of the solvent gave the crude product as a yellowish powder. Pure product **1** was obtained in 77% yield (179 mg) by recrystallization from CH_3CN/CH_2Cl_2 (2:1). ^{1}H NMR (300 MHz, CD_3CN): δ 8.49 (s, 3 H, Py-*H*), 7.51−7.12 (m, 10 H, Ar-*H*), 2.52 (s, 6 H, N=C*Me*). ^{13}C NMR (CD_3CN, ^{1}H gated decoupled): δ 164.79 (N=C), 148.83 (P_y-C_o), 147.56 (Ar-C_{ip}), 142.52 (Ar-C_o), 129.33 (Ar-C_p), 128.35 (Py-C_p), 126.02 (Py-C_m), 121.05 (Ar-C_m), 17.78 (N=C-*Me*). IR (KBr, cm^{-1}): 3089 (w), 3019 (w), 2970 (w), 2920 (w), 2247 (w), 1643 (s), 1594 (s), 1485 (s), 1448 (m), 1368 (s), 1247 (s), 1225 (s), 1185 (w), 1148 (w), 1011 (w), 906 (w), 816 (s), 775 (s), 697 (s), 573 (w), 532 (w). Elem anal. calcd for $C_{21}H_{19}N_3HgCl_2\cdot 1.5CH_3CN$: C, 44.59; H, 3.66; N, 9.75. Found: C, 44.19; H, 3.60; N, 9.44.

Synthesis of 2,6-Bis[1-(2,6-diisopropylphenylimino)ethyl]pyridineHgCl$_2$ (2). Complex **2** was prepared in the same way as described for **1**. Yield: 78%. ^{1}H NMR (300 MHz, CD_3CN): δ 8.52 (s, 3 H, Py-*H*), 7.26−7.18 (m, 6 H, Ar-*H*), 2.87 (sept, J = 6.8 Hz, 4 H, C*H*Me$_2$), 2.39 (s, 6 H, N=C*Me*), 1.23 (dd, J = 6.8 Hz, 24 H, CH*Me*$_2$). IR (KBr, cm^{-1}): 3088 (w), 3059 (w), 2960 (s), 2925 (m), 2865 (m), 1638 (s), 1581 (s), br 1455 (s), 1366 (s), 1329 (m), 1301 (m), 1244 (s), 1202 (s), 1105 (m), 1056 (m), 978 (w), 936 (m), 819 (m), 793 (s), 774 (s), 759 (w), 715 (w), 634 (w), 554 (w). Elem anal. calcd for $C_{33}H_{43}N_3HgCl_2$: C, 52.62; H, 5.75; N, 5.58. Found: C, 52.88; H, 5.96; N, 5.89.

Synthesis of 2,6-Bis[1-(2,6-dimethylphenylimino)ethyl]pyridineHgCl$_2\cdot$CH$_3$CN (3). Complex **3** was prepared in the same way

(14) (a) Small, B. L.; Brookhart, M.; Bennett, A. M. A. *J. Am. Chem. Soc.* **1998**, *120*, 4049. (b) Britovsek, G. J. P.; Gibson, V. C.; Kimberley, B. S.; Maddox, P. J.; McTavish, S. J.; Solan, G. A.; White, A. J. P.; Williams, D. J. *J. Chem. Soc., Chem. Commun.* **1998**, 849. (c) Gibson, V. C.; Redshaw, C.; Solan, G. A. *Chem. Rev.* **2007**, *107*, 1745.

(15) (a) Bennett, A. M. A. *Chemtech* **1999**, *29*, 24. (b) Lttel, S. D.; Johnson, L. K. *Chem. Rev.* **2000**, *100*, 1169. (c) Small, B. L.; Marcucci, A. J. *Organometallics* **2001**, *20*, 5738. (d) Pelascini, F.; Wesolek, M.; Peruch, F.; Lutz, P. J. *Eur. J. Inorg. Chem.* **2006**, 4309.

(16) (a) Abu-Surrah, A. S.; Lappalainen, K.; Piirone, U.; Lehmus, P.; Repo, T.; Leskelä, M. *J. Organomet. Chem.* **2002**, *648*, 55. (b) Gibson, V. C.; Spitzmesser, S. K. *Chem. Rev.* **2003**, *103*, 283.

(17) (a) Mahmoudkhani, A. H.; Langer, V.; Casari, B. M. *Acta Crystallogr.* **2001**, *E57*, m393. (b) Fan, R.-Q.; Wang, P.; Yang, Y.-L.; Lv, Z.-W. *Acta Crystallogr.* **2007**, *E63*, m2501. (c) Jia, W. L.; Liu, Q. D.; Song, D; Wang, S. *Organometallics* **2003**, *22*, 321.

(18) Zhong, J. Z.; Wang, F. *Acta Acad. Med. Jiangxi* **1999**, *39*, 93.

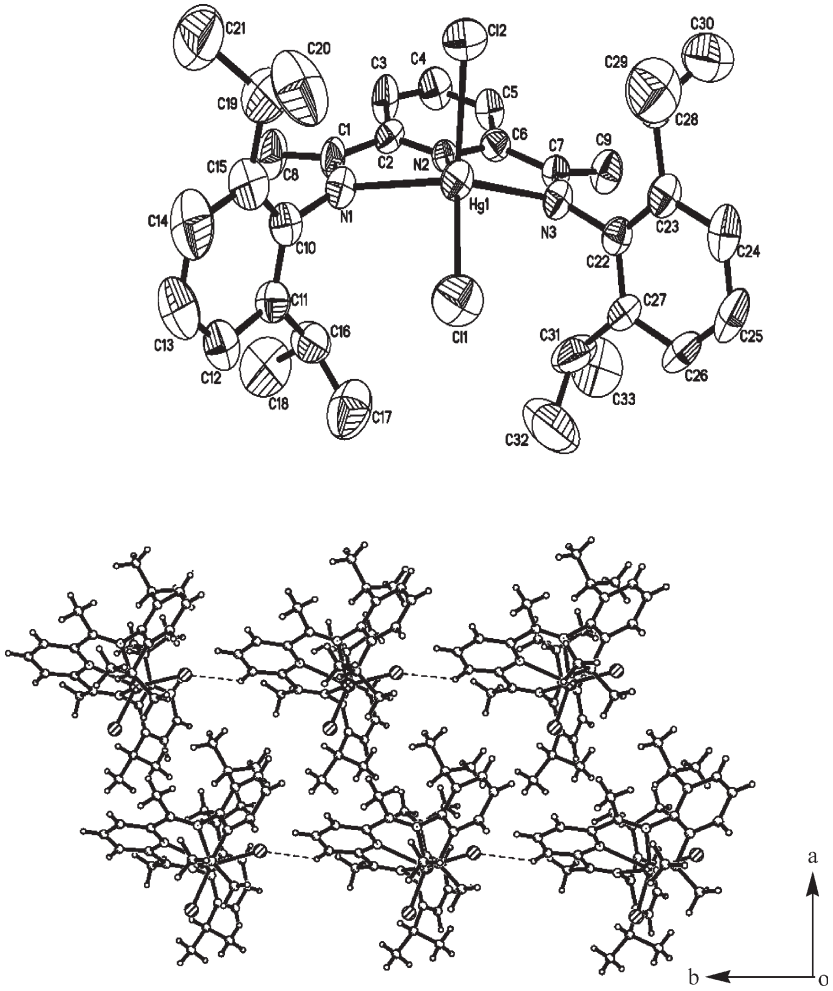

Figure 2. Top: Molecular structure of complex **2**. Bottom: Packing diagram of complex **2** along the *c* axis. Hydrogen bonds are indicated by dashed lines.

as described for **1**. Yield: 80%. ^{1}H NMR (300 MHz, CD_3CN): δ 8.54 (s, 3 H, Py-*H*), 7.22−6.87 (m, 6 H, Ar-*H*), 2.41 (s, 6 H, N=C*Me*), 2.19 (s, 12 H, C*Me*). IR (KBr, cm^{-1}): 3084 (w), 3019 (w), 2960 (w), 2920 (w), 1646 (s), 1583 (s), 1466 (s), 1440 (m), 1371 (s), 1251 (s), 1215 (s), 1093 (w), 1036 (w), 979 (w), 919 (w), 817 (m), 781 (m), 737 (w), 697 (w), 580 (w). Elem anal. calcd for $C_{25}H_{27}N_3HgCl_2 \cdot CH_3CN$: C, 47.55; H, 4.43; N, 8.21. Found: C, 47.38; H, 4.51; N, 8.15.

Synthesis of 2,6-Bis[1-(2-methylphenylimino)ethyl]pyridineHgCl$_2$·CH$_3$CN (4). Complex **4** was prepared in the same way as described for **1**. Yield: 82%. ^{1}H NMR (300 MHz, CD_3CN): δ 8.50 (s, 3 H, Py-*H*), 7.30−6.61 (m, 8 H, Ar-*H*), 2.43 (s, 6 H, N=C*Me*), 2.22 (s, 6 H, C*Me*). IR (KBr, cm^{-1}): 3078 (w), 3019 (w), 2920 (w), 1646 (s), 1581 (s), 1482 (s), 1457 (m), 1368 (m), 1249 (s), 1225 (s), 1200 (m), 1113 (w), 1044 (w), 1011 (w), 816 (s), 786 (s), 753 (s), 718 (m), 666 (w), 443 (m). Elem anal. calcd for $C_{23}H_{23}N_3HgCl_2 \cdot CH_3CN$: C, 45.91; H, 4.01; N, 8.57. Found: C, 45.68; H, 4.38; N, 8.29.

Synthesis of 2,6-Bis[1-(4-methylphenylimino)ethyl]pyridineHgCl$_2$·CH$_3$CN (5). Complex **5** was prepared in the same way as described for **1**. Yield: 85%. ^{1}H NMR (300 MHz, CD_3CN): δ 8.25 (s, 3 H, Py-*H*), 7.11−6.84 (m, 8 H, Ar-*H*), 2.32 (s, 6 H, N=C*Me*), 2.20 (s, 6 H, C*Me*). IR (KBr, cm^{-1}): 3079 (w), 3025 (w), 2915 (w), 2860 (w), 1638 (m), 1583 (m), 1505 (s), 1458 (m), 1368 (m), 1250 (s), 1226 (s), 1104 (w), 1013 (w), 842 (m), 813 (m), 762 (w), 734 (s), 707 (w), 630 (w), 542 (w), 514 (w). Elem anal. calcd for $C_{23}H_{23}N_3HgCl_2 \cdot CH_3CN$: C, 45.91; H, 4.01; N, 8.57. Found: C, 45.88; H, 4.11; N, 8.75.

Synthesis of 2,6-Bis[1-(2,4,6-trimethylphenylimino)ethyl]pyridineHgCl$_2$·CH$_3$CN (6). Complex **6** was prepared in the same way as described for **1**. Yield: 80%. ^{1}H NMR (300 MHz, CD_3CN): δ 8.60 (s, 3 H, Py-*H*), 6.91 (s, 4 H, Ar-*H*), 2.50 (s, 6 H, N=C*Me*), 2.24 (s, 6 H, C*Me*), 2.01 (s, 12 H, C*Me*). IR (KBr, cm^{-1}): 3086 (w), 2950 (w), 2918 (m), 2860 (w), 2737 (w), 1642 (s), 1584 (s), 1474 (s), 1435 (m), 1370 (m), 1247 (s), 1222 (s), 1157 (w), 1098 (w), 1007 (w), 846 (s), 807 (s), 736 (w), 645 (w), 561 (w). Elem anal. calcd for $C_{27}H_{31}N_3HgCl_2 \cdot CH_3CN$: C, 49.05; H, 4.83; N, 7.89. Found: C, 48.98; H, 4.81; N, 7.75.

Synthesis of 2,6-Bis[1-(2,6-diethylphenylimino)ethyl]pyridineHgCl$_2$·CH$_3$CN (7). Complex **7** was prepared in the same way as described for **1**. Yield: 82%. ^{1}H NMR (300 MHz, CD_3CN): δ 8.47 (s, 3 H, Py-*H*), 7.22−7.18 (m, 6 H, Ar-*H*), 2.68 (q, J = 6.8 Hz, 8 H, Ar−CH_2Me), 2.36 (s, 6 H, N=C*Me*), 1.09 (t, J = 6.8 Hz, 12 H, Ar−CH$_2$*Me*). IR (KBr, cm^{-1}): 3067 (w), 2964 (s), 2938(m), 2880 (m), 1622 (m), 1589 (s), 1447 (s), 1369 (s), 1319 (m), 1271 (s), 1213 (s), 1109 (w), 1038 (w), 985 (w), 868 (w), 810 (s), 771 (s), 745 (w), 641 (w), 550 (w). Elem anal. calcd for $C_{29}H_{35}N_3HgCl_2$: C, 49.97; H, 5.06; N, 6.03. Found: C, 50.08; H, 5.31; N, 6.25.

X-Ray Crystallography. The single-crystal X-ray diffraction data for complexes **1**−**6** were collected on a Rigaku R-AXIS RAPID IP or a Bruker Smart Apex CCD diffractometer equipped with graphite-monochromated Mo Kα radiation (λ = 0.71073 Å), operating at 293 ± 2 K. The structures were solved by direct methods and refined by full-matrix

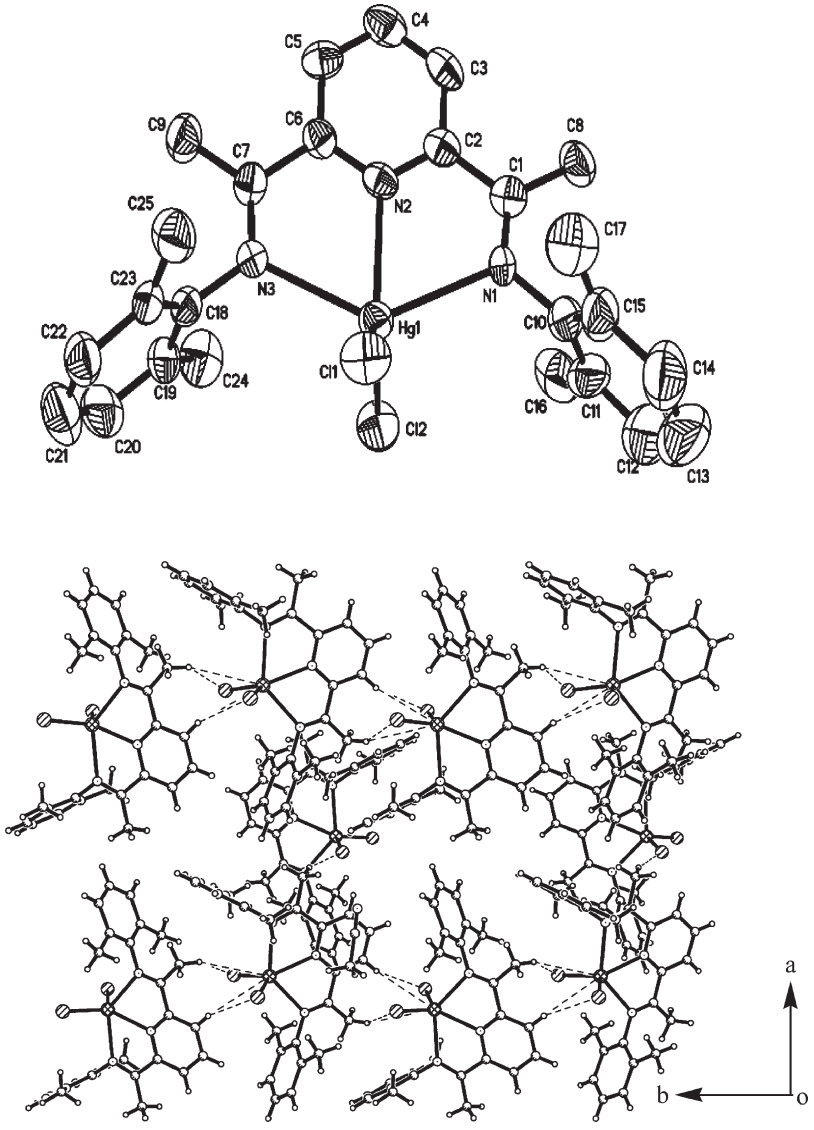

Figure 3. Top: Molecular structure of complex **3** (the CH_3CN molecule has been omitted for clarity). Bottom: Packing diagram of complex **3** along the *c* axis. Hydrogen bonds are indicated by dashed lines.

least-squares based on F^2 using the SHELXTL 5.1 software package.[19] The hydrogen atoms residing on the carbon atoms were located geometrically. All non-hydrogen atoms were refined anisotropically. Crystallographic data are given in Table 1. The CCDC reference numbers for complexes **1**−**6** are 232414, 232419, 232420, 232415, 720498, and 720499, respectively. Crystallographic data are given in Table 1.

Results and Discussion

Synthesis. The bis(imino)pyridine mercury complexes **1**−**7** were synthesized in good yield (ca. 77−85%) as air-stable yellowish solids by reactions of the corresponding bis(imino)pyridyl ligands with $HgCl_2$ in CH_3CN solution at room temperature (Scheme 1). All compounds were characterized by ^1H NMR, UV/vis, and IR spectroscopies as well as elemental analyses. Molecular structures of complexes **1**−**6** were determined by single-crystal X-ray diffraction analyses.

(19) *SHELXTL NT Crystal Structure Analysis Package*, version 5.10; Bruker AXS, Analytical X-ray System: Madison, WI, 1999.

Crystal Structures. Crystals of **1**−**6** suitable for X-ray structural determination were grown from an acetonitrile/dichloromethane (2:1) solution (**1**, **3**, **4**, and **5**), from a concentrated dichloromethane solution (**2**), or from a concentrated tetrahydrofuran solution (**6**). The molecular structures of complexes **1**−**6** are shown in Figures 1−6, respectively, and selected bond lengths and angles are presented in Table 2.

Complexes **1**, **2**, **3**, **5**, and **6** possess structures with approximate C_s symmetry about a plane bisecting the central pyridine ring and containing the mercury atom and two chlorine atoms, while complex **4** adopts C_2 symmetry. The central mercury atom in **1**−**6** is coordinated to five groups, and the geometry about the mercury atom is a distorted trigonal bipyramid, with the equatorial plane defined by the N(2)(pyridine), Cl(1), and Cl(2) atoms and the N(1) and N(3)(imino) atoms in the axial position, in which Hg−Cl(2) bond distances are significantly longer than that of Hg−N(2); moreover, Hg−N(3) bond distances are still longer than that of Hg−N(1). There are two independent complex molecules and three

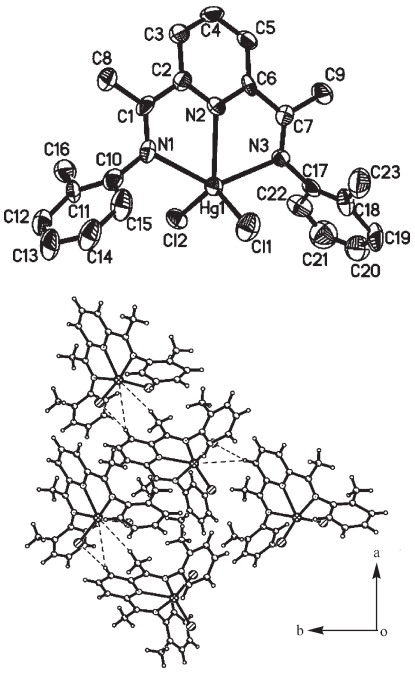

Figure 4. Top: Molecular structure of complex **4** (the other molecule and CH_3CN molecules have been omitted for clarity). Bottom: Packing diagram of complex **4** along the *c* axis. Hydrogen bonds are indicated by dashed lines.

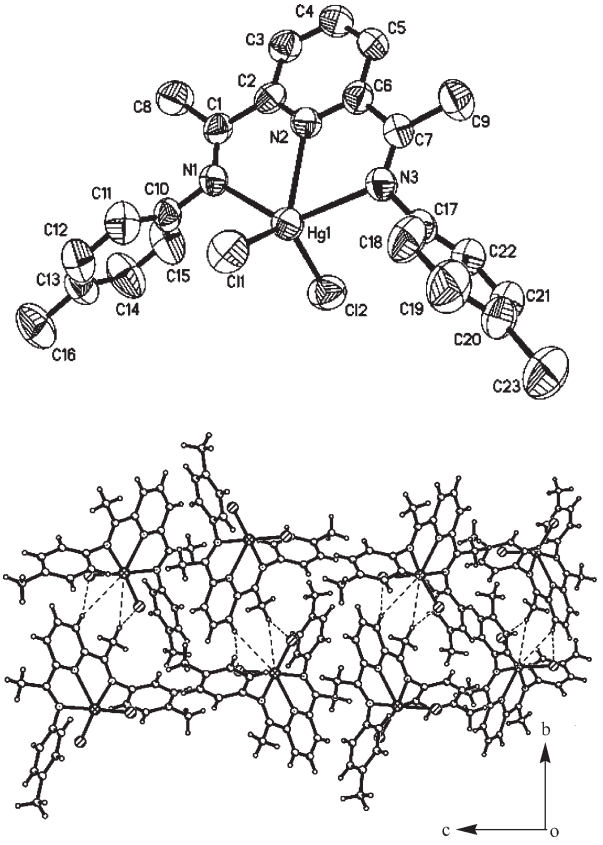

Figure 5. Top: Molecular structure of complex **5** (the CH_3CN molecule has been omitted for clarity). Bottom: Packing diagram of complex **5** along the *a* axis. Hydrogen bonds are indicated by dashed lines.

acetonitrile molecules in the asymmetric unit in mercury complex **1**. Complexes **3** and **5** contain one independent molecule and one acetonitrile molecule, whereas there are two independent molecules and two acetonitrile molecules in the asymmetric unit in mercury complexes **4** and **6**, respectively. The dihedral angles in one molecule in **1** between the phenyl rings and the plane formed by the three coordinated nitrogen atoms are 75.6(4) and 80.4 (5)°, larger than those in the other molecule [60.0(3) and 66.5(3)°, respectively]. The dihedral angles in **2**−**6** ranging between the phenyl rings and plane formed by three coordinated nitrogen atoms are 75.3(4) and 89.3(3)°. The dihedral angles between the two phenyl rings are 73.4(4)° and 83.0(4)° in the two molecules in **1**. The dihedral angles between the two phenyl rings are oriented essentially orthogonally in **2**−**6** [ranging between 80.6(3)° and 89.0(2)°]. The mean deviation of the mercury atoms in **1**−**6** from the equatorial planes is 0.015, 0.032, 0.019, 0.011, 0.012, and 0.022 Å (0.014, 0.012, and 0.010 Å for the other molecule in **1**, **4** and **6**, respectively), respectively, and the axial Hg−N(imino) bonds subtend angles of 134.4(3)°, 126.6(2)°, 135.6(2)°, 134.8(3)°, 133.9(1)°, and 135.3(2)° , respectively [135.2 (1)°, 135.5(3)°, and 134.3(2)° for the other molecule in **1**, **4**, and **6**, respectively]. The mercury atoms in **1**−**6** deviate by 0.113, 0.740, 0.120, 0.054, 0.032, and 0.017 Å, respectively (0.110, 0.001, and 0.180 Å for the other molecule in **1**, **4**, and **6**, respectively), from the coordinated plane. The Hg−N (pyridine) bonds in **1**−**6** range from 2.354(1) to 2.399-(6) Å, while the distances between the mercury atom and the imino nitrogen atoms in the six complexes are almost the same [2.429(9) and 2.443(9) Å] in **1** [2.449(1) and 2.477(1) Å for the other molecule in **1**], [2.514(6) and 2.533(7) Å] **2**, [2.475(5) and 2.487(6) Å] **3**, [2.421(9) and 2.457(9) Å] **4** [2.424(10) and 2.443(9) Å for the other molecule in **4**], [2.461(4) and 2.452(4) Å] **5**, and [2.490(7) and 2.457(6) Å] **6** [2.498(6) and 2.450(6) Å for the other molecule in **6**]. In each complex, the Hg−N(pyridine) bond is significantly shorter than the Hg−N(imino) bonds, with the formal double-bond character of the imino linkages N(1)−C(1) and N(3)−C(7) being retained [C=N distances in the range 1.249(13)−1.324(11) Å]. There are no intermolecular packing features of interest in any of the six complexes. However, the structures of complexes **1**−**6** are stabilized by the hydrogen bonds between the Cl atom and C atoms of the adjacent complexes (Figures 1−6 bottom), as indicated by the distances of Cl···C, 3.453−3.828 Å, and the bond angles of Cl···H···C, 133.65−165.87°, which are similar to results from the literature reported previously.[17a,17b] The Cl···C bond distances and Cl···H···C bond angles are listed in Table 3.

Luminescent Properties. Table 4 presents the absorption and emission data for the new complexes **1**−**7** in a dichloromethane solution and in the solid state at room temperature together with those of ligands L^1−L^7. The seven complexes show two main absorption bands (Figures 7), which are similar to those in ligands L^1−L^7 in the UV region. The electronic absorption spectra of the complexes show low energy absorption bands at ca. 346−364 nm (329−347 nm for ligands L^1−L^7) and higher energy absorption bands at ca. 288−303 nm (281−300 nm for ligands L^1−L^7), attributed to ligand-centered $\pi \rightarrow \pi^*$ transitions. The electronic absorption spectra of the complexes compared with ligands are red-shifted, for the metal perturbed intraligand $\pi \rightarrow \pi^*$ transition of the

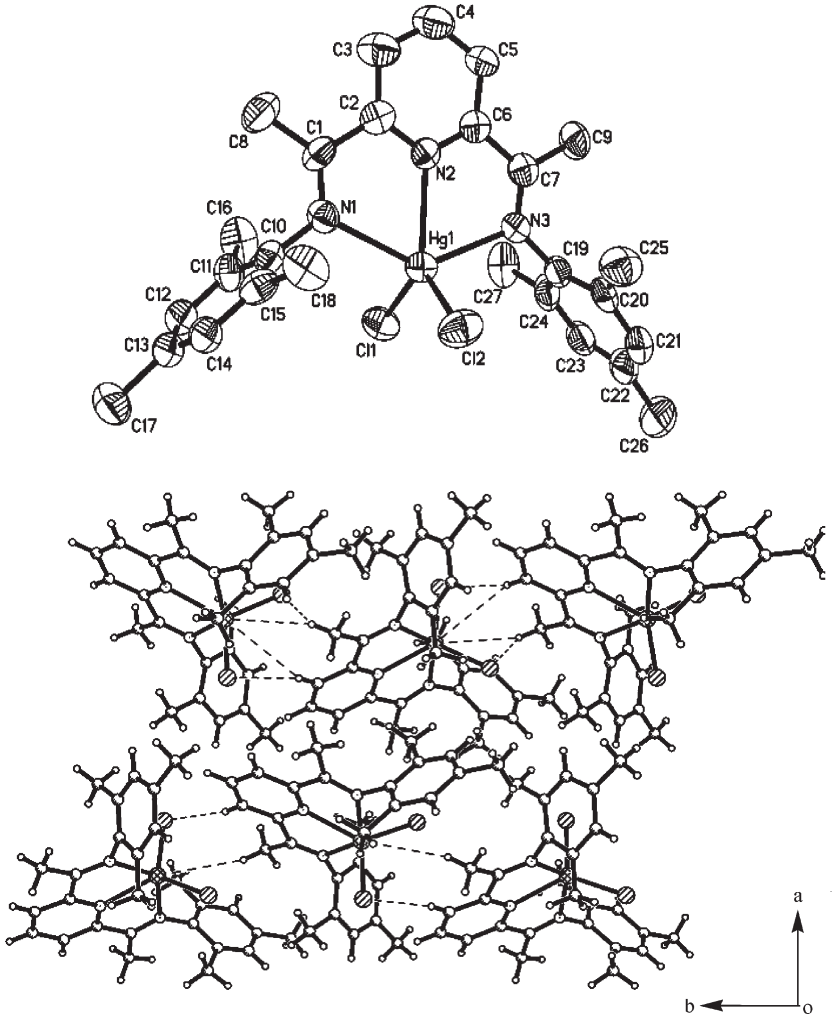

Figure 6. Top: Molecular structure of complex **6** (the other molecule and CH_3CN molecules have been omitted for clarity). Bottom: Packing diagram of complex **6** along the *c* axis. Hydrogen bonds are indicated by dashed lines.

Table 2. Selected Bond Lengths (Å) and Angles (deg) for **1**−**6**

	1		**2**	**3**	**4**		**5**	**6**	
	molecule1-1	molecule1-A			molecule4-1	molecule4-A		molecule7-1	molecule7-A
Hg−N(2)	2.382(8)	2.354(1)	2.399(6)	2.354(6)	2.376(9)	2.382(8)	2.387(4)	2.370(6)	2.387(6)
Hg−N(1)	2.429(9)	2.449(1)	2.514(6)	2.475(5)	2.421(9)	2.424(10)	2.461(4)	2.490(7)	2.498(6)
Hg−Cl(1)	2.389(3)	2.398(1)	2.365(3)	2.414(2)	2.396(4)	2.416(3)	2.416(1)	2.430(2)	2.423(2)
Hg−N(3)	2.443(8)	2.477(1)	2.533(7)	2.487(6)	2.457(9)	2.443(9)	2.452(4)	2.457(6)	2.450(6)
Hg−Cl(2)	2.434(3)	2.427(1)	2.418(3)	2.412(2)	2.420(3)	2.426(3)	2.424(1)	2.442(2)	2.445(2)
N(1)−C(1)	1.271(14)	1.281(1)	1.266(11)	1.259(10)	1.317(11)	1.317(11)	1.265(6)	1.272(9)	1.286(9)
N(3)−C(7)	1.249(13)	1.275(10)	1.291(11)	1.275(9)	1.300(14)	1.324(11)	1.264(6)	1.265(9)	1.287(9)
N(2)−Hg−N(1)	67.4(3)	67.6(1)	65.7(2)	67.4(2)	67.6(3)	67.9(3)	67.1(1)	67.6(2)	67.1(2)
N(2)−Hg−Cl(1)	125.8(2)	129.1(1)	134.5(2)	122.1(2)	119.8(2)	124.5(2)	120.2(1)	121.7(2)	127.0(2)
N(1)−Hg−Cl(1)	104.7(2)	101.9(1)	98.3(2)	102.8(2)	100.5(2)	101.7(2)	101.2(1)	99.8(2)	102.7(2)
N(2)−Hg−N(3)	67.1(3)	67.7(1)	65.4(2)	68.3(2)	67.2(3)	67.6(3)	66.8(1)	67.7(2)	67.6(2)
N(1)−Hg−N(3)	134.4(3)	135.2(1)	126.6(2)	135.6(2)	134.8(3)	135.5(3)	133.9(1)	135.3(2)	134.3(2)
Cl(1)−Hg−N(3)	104.1(2)	103.3(1)	100.9(2)	97.5(2)	100.1(2)	103.1(2)	100.7(1)	102.9(2)	100.0(2)
N(2)−Hg−Cl(2)	109.8(2)	109.1(1)	94.4(2)	115.7(2)	113.6(2)	115.9(2)	115.2(1)	118.8(2)	114.4(2)
N(1)−Hg−Cl(2)	94.5(2)	98.5(1)	101.1(2)	99.9(2)	98.4(2)	101.0(2)	100.4(1)	100.9(2)	99.5(2)
Cl(1)−Hg−Cl(2)	124.4(1)	121.8(1)	131.0(1)	122.1(1)	126.6(1)	119.6(1)	124.6(1)	119.5(8)	118.5(8)
N(3)−Hg−Cl(2)	97.5(3)	98.8(1)	102.6(2)	102.0(2)	100.7(2)	98.1(2)	99.6(1)	100.6(2)	103.5(2)

bis(imino)pyridyl unit. The energy trend of this band for the complex **1**−**7** series is found to follow the order **5** < **6** < **3** < **4**, **7** < **2** < **1** (similar to ligands L^1−L^7). It is very interesting that the electron-donating ability of the alkyl group (2,4,6-trimethylphenyl > 2,6-dimethylphenyl > 2-methylphenyl, 2,6-diethylphenyl > 2,6-diisopropylphenyl > phenyl) is in the line with the energy trend, with the exception of complex **5**. Complex **5** shows that the lowest absorption energy attributable to lower steric hindrance on the *p*-methyl-substituted phenyl

ring of the bis(imino)pyridyl metal complex leads to a highly coplanar situation and an absorption energy red shift.

Complexes **1**−**7** have blue emission in a degassed CH_2Cl_2 solution at room temperature, with λ_{max} = 395, 400, 407, 403, 427, 415, and 403 nm, respectively (Figure 8; λ_{max} = 368, 375, 381, 378, 405, 388, and 380 nm, for L^1−L^7). Similar to the electronic absorption data, their emission energies are found to depend on the electron donation of the alkyl substituents on the aryl rings of the bis(imino)pyridyl ligand and steric effects. For the complex **1**−**7** series, an emission energy trend in the order **5** < **6** < **3** < **4**, **7** < **2** < **1** is observed, again in line with the electron-donating ability of the alkyl and with steric effects. The quantum yields of all compounds have been determined in solution (Table 4). It was found that the quantum yields of Hg(II) complexes **1**−**7** are slightly higher than those of free ligands L^1−L^7 and are lower than those of their Zn(II) complexes.[15b] These results can be easily understood considering the following factors: The chelation of the ligand to the metal center increases the rigidity of the ligand and thus reduces the loss of energy by thermal vibrational decay and therefore increases the emission efficiency. On the other hand, the Hg(II) cation and the chloride anions can quench the fluorescence and result in luminescence decay. These emission bands are dominated by fluorescence. The fluorescence decay lifetimes of **1**−**7** were found to range from 2.11 to 2.95 ns (0.62−0.95 ns for ligands L^1−L^7; Table 4). However, in the solid state at room temperature, complexes **1**−**7** exhibit a bright greenish-blue color emission band with an emission maximum at λ_{max} = 485, 486, 488, 486, 498, 492, and 486 nm, respectively (λ_{max} = 471, 475, 480, 476, 485, 480, and 475 nm for L^1−L^7), red-shifted about 80 nm (ca. 100 nm for L^1−L^7) from that of the emission in solution (Figure 9). This dramatic red shifts of the emission energy of complexes **1**−**7** from solution to solid are probably caused by the intermolecular hydrogen bonds in solid-state complexes **1**−**7**, which effectively decreases the energy gap. The existence of intermolecular hydrogen bonds in complexes **1**−**6**, as shown by the crystal structures, may be a factor contributing to the red shift.[17c]

To further understand the origin of the red shift of the absorption energy from the free ligand to the complex, we

Table 3. Hydrogen-Bond Geometry (Å, deg) for **1**−**6**

	D−H···A	D····A	D−H···A
1	Cl1−H···C20	3.681	138.23
	Cl2−H···C12	3.742	154.16
	Cl2−H···C12A	3.716	160.42
	Cl2−H···C3A	3.621	159.67
	Cl1A−H···C9	3.681	149.26
	Cl2A−H···C5	3.650	164.27
2	Cl1−H···C3	3.453	133.65
3	Cl1−H···C3	3.643	162.42
	Cl1−H···C9	3.828	163.45
	Cl2−H···C8	3.651	141.77
4	Cl1−H···C23A	3.763	147.22
	Cl2−H···C21	3.625	146.44
	Cl2−H···C3A	3.621	161.84
	Cl2A−H···C3	3.662	163.31
5	Cl1−H···C8	3.761	147.15
	Cl1−H···C9	3.686	147.37
	Cl2−H···C5	3.652	165.02
6	Cl1−H···C9	3.636	141.95
	Cl2−H···C5	3.643	159.66
	Cl2A−H···C5A	3.728	165.87

Table 4. Photoluminescent Data for **1**−**7** and L^1−L^7[a]

compound	absorption (nm) ε/dm^3 mol^{-1} cm^{-1}	excitation (λ_{max}, nm)	emission (λ_{max}, nm)	quantum yields (Φ)[b]	decay lifetime (τ, ns)	conditions
1	288 (15522), 346 (3017)		395	0.028	2.11	CH_2Cl_2, 298 K
		330	485			solid, 298K
2	293 (15590), 352 (3221)		400	0.032	2.25	CH_2Cl_2, 298 K
		330	486			solid, 298K
3	300 (15986), 360 (3491)		407	0.037	2.88	CH_2Cl_2, 298 K
		330	488			solid, 298K
4	296 (15716), 355 (3356)		403	0.034	2.60	CH_2Cl_2, 298 K
		330	486			solid, 298 K
5	303 (15907), 364 (5973)		427	0.035	2.65	CH_2Cl_2, 298 K
		330	498			solid, 298 K
6	302 (15846), 360 (2661)		415	0.042	2.95	CH_2Cl_2, 298 K
		330	492			solid, 298 K
7	296 (15741), 356 (2559)		403	0.032	2.28	CH_2Cl_2, 298 K
		330	486			solid, 298 K
L^1	281 (16025), 329 (7485)[c]		368[c]	0.005	0.62	CH_2Cl_2, 298 K
		330	471[c]			solid, 298 K
L^2	284 (16180), 334 (7640)[c]		375[c]	0.008[d]	0.76[d]	CH_2Cl_2, 298 K
		330	475[c]			solid, 298 K
L^3	291 (16528), 340 (7998)[c]		381[c]	0.009[d]	0.89[d]	CH_2Cl_2, 298 K
		330	480[c]			solid, 298 K
L^4	287 (16335), 337 (7843)[c]		378[c]	0.008	0.73	CH_2Cl_2, 298 K
		330	476[c]			solid, 298 K
L^5	300 (26463), 347 (18838)		405	0.008	0.80	CH_2Cl_2, 298 K
		330	485			solid, 298 K
L^6	296 (21090), 342 (12340)		388	0.012	0.95	CH_2Cl_2, 298 K
		330	480			solid, 298 K
L^7	287 (16418), 338 (7862)		380	0.009	0.80	CH_2Cl_2, 298 K
		330	475			solid, 298 K

[a] Concentration: [M] = 1×10^{-5} M. [b] Determined using quinine sulfate in 0.1 M sulphuric acid as a standard. [c] Photoluminescent data of L^1−L^4 from ref 15. [d] Photoluminescent data of L^1−L^4 from ref 15.

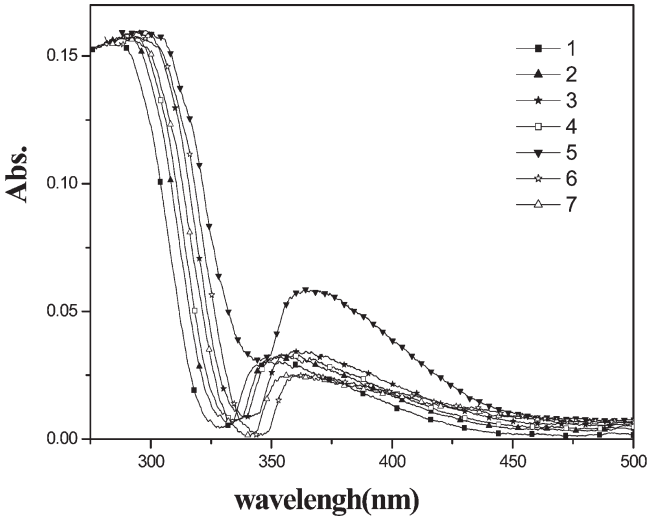

Figure 7. UV−vis absorption spectra of complexes **1**−**7**.

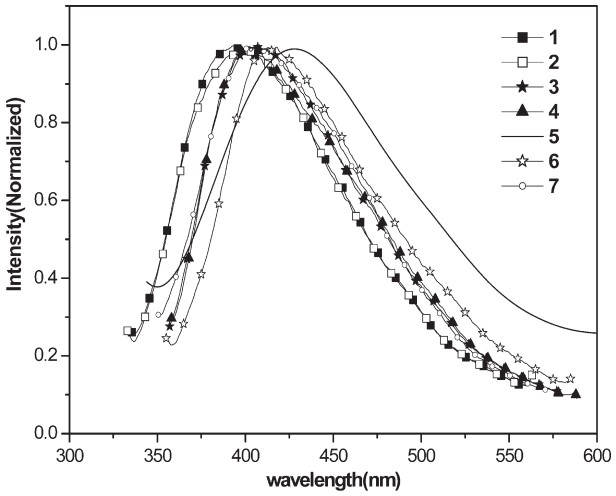

Figure 8. Emission spectra of complexes **1**−**7** in CH_2Cl_2 solution at 298 K.

performed ab initio calculations (ADF2008)[20] for the free ligand L^2 and complex **2** based on the time-dependent density functional theory (TD-DFT) GGA-PW91 method, with the TZP basis set for all atoms.[21] The geometric parameters obtained from X-ray diffraction analyses were fully optimized in conjunction with the COSMO[22] solvent model (CH_2Cl_2, $\varepsilon = 8.9$), and the symmetries of both compounds are a little enhanced, that is, C_2 and C_s for the L^2 and complex **2**, respectively. The properties of the significant transitions are reported in Table 5, and the qualitative MO diagram and shapes of the spectroscopically relevant molecular orbitals are plotted in Figure 10.

(20) *ADF 2008.01*; Department of Theoretical Chemistry, Vrije Universiteit: Amsterdam.(a) Baerends, E. J.; Ellis, D. E.; Ros, P. *Chem. Phys.* **1973**, *2*, 41. (b) Versluis, L.; Ziegler, T. *J. Chem. Phys.* **1988**, *88*, 322. (c) Te Velde, G.; Baerends, E. J. *J. Comput. Phys.* **1992**, *99*, 84. (d) Baerends, E. J. *Theor. Chem. Acc.* **1998**, *99*, 391.

(21) The internal electrons (1s for Cl, C, and N; 1s to 4d for Hg) were described by means of single Slate functions. The quasi-relativistic forzen core shells generated by the auxiliary program DIRAC were used to correct the core potential within the ZORA formalism.

(22) (a) Klamt, A.; Schüürmann, G. *J. Chem. Soc., Perkin Trans.* **1993**, *2*, 799. (b) Klamt, A. *J. Chem. Phys.* **1995**, *99*, 2224.

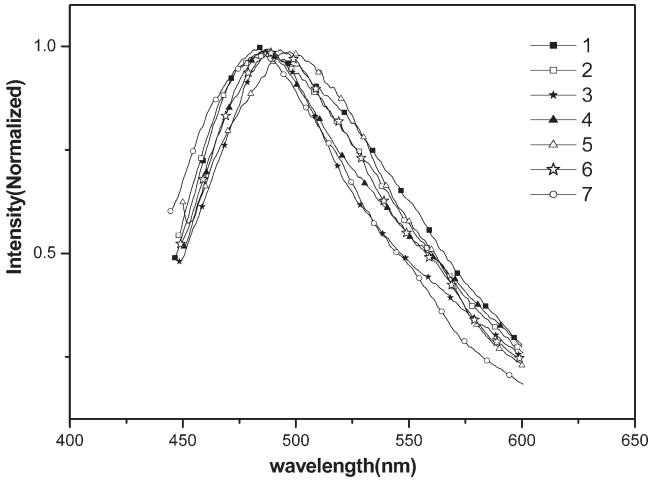

Figure 9. Emission spectra of complexes **1**−**7** in the solid state at 298 K.

Table 5. Primary Electron Transitions of L^2 and **2** at the TD−DFT/TZP Level

compound	E_{ge} (ev)	λ (nm)	f_{os}	major contributions
L^2	4.2703	290.30	0.0770	HOMO−6 → LUMO (43.5%)
	3.8633	320.93	0.0170	HOMO−4 → LUMO + 1 (91.7%)
2	3.4068	363.93	0.0515	HOMO−1 → LUMO + 2 (96.1%)
	3.3919	365.53	0.0011	HOMO → LUMO + 2 (72.2%)

For ligand L^2, the electron transitions are complicated, and there are many transitions with small oscillator strengths that can be obtained. It is interesting to note that the intense bands of both ∼280 and ∼330 nm in the experiments are well reproduced, that is, respectively 290.30 nm (HOMO−6 → LUMO) and 320.93 nm (HOMO−4 → LUMO + 1) in computations, and mainly come from $\pi \rightarrow \pi^*$ transitions in the center pyridyl ring. In contrast, the electron transitions for complex **2** are relatively simple and dominantly come from the frontier molecular orbitals. As can be seen, the electron densities of HOMO−1 and HOMO for complex **2** are located toward the conjugated C=N bridge and the phenyl ring, while those of LUMO + 2 are located on the $HgCl_2$ subunit in the center part of the whole molecule. Computationally, the intense absorption band (∼365 nm) for complex **2** compares well with the experimental one at ∼350 nm; however, the band at ∼290 nm in the experiment is difficult to predict and might be attributed to the insufficiency of the TD-DFT method employed.[23] As given in Figure 10, the intense bands including 363.93 nm originating from an almost pure HOMO−1 → LUMO + 2 (54A″ → 67A′) and 365.53 nm coming mainly from HOMO → LUMO + 2 (65A′ → 67A′) are characteristic for metal-to-ligand charge transfer excitation from the peripheral phenyl ring to the center Hg/Cl atoms. Obviously, the electron densities on the metal atom in 67A′ (LUMO + 2) are not small, which indicates that Hg(II) plays an important role of electronic transmission during the transition. In addition, the shift of absorption energy of the complex in comparison to the free ligand is consistent with the experimental observation.

(23) Cramariuc, O.; Hukka, T. I.; Rantala, T. T.; Lemmetyinen, H. *J. Phys. Chem. A* **2006**, *110*(45), 12470.

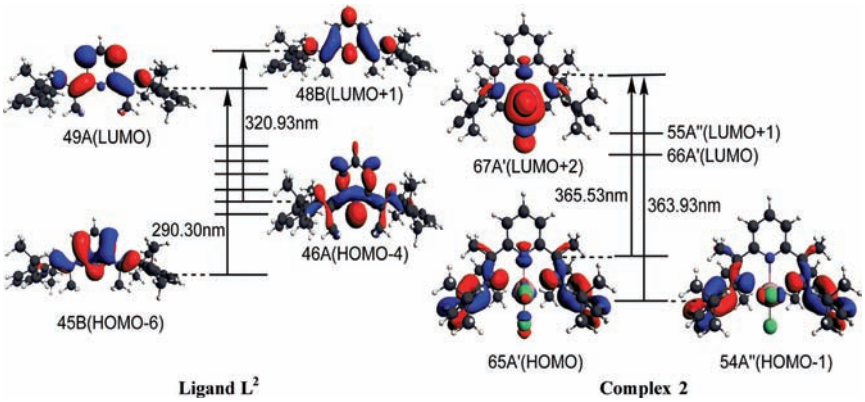

Figure 10. Qualitative MO diagram and shapes of the spectroscopically relevant molecular orbitals. The orbital labels correspond to those in Table 5.

Conclusion

A series of mercury(II) bis(imino)pyridyl complexes has been synthesized and characterized. Complexes **1**−**7** have fluorescent emission at 395−427 nm in a dichloromethane solution at room temperature. Complexes **1**−**7** have fluorescent emission bands in the solid state at room temperature, with λ_{max} = 485, 486, 488, 486, 498, 492, and 486 nm for **1**−**7**, respectively. Their luminescent properties show that they are a new class of luminescent metal compounds with potential applications in optoelectronic devices.

Acknowledgment. This work was supported by the National Natural Science Foundation of China (Grant Nos. 20771030, 20671025, and 60778019), Young Foundation of Heilongjiang Province in China (QC06C029), and The Research Fund for the Doctoral Program of Higher Education (20070213005). We thank Dr. Yongqing Qiu in Northeast Normal University for providing quantum chemical calculations.

Supporting Information Available: A crystallographic information file (CIF) is provided. This material is available free of charge via the Internet at http://pubs.acs.org.